ISSN 0252-1075
Contribution from IITM
Research Report No. RR-146
ESSO/IITM/MM/SR/02(2019)/197

Performance of Very High Resolution Global Forecast System Model (GFS T1534) at 12.5km over Indian Region during 2016-2017 Monsoon Seasons

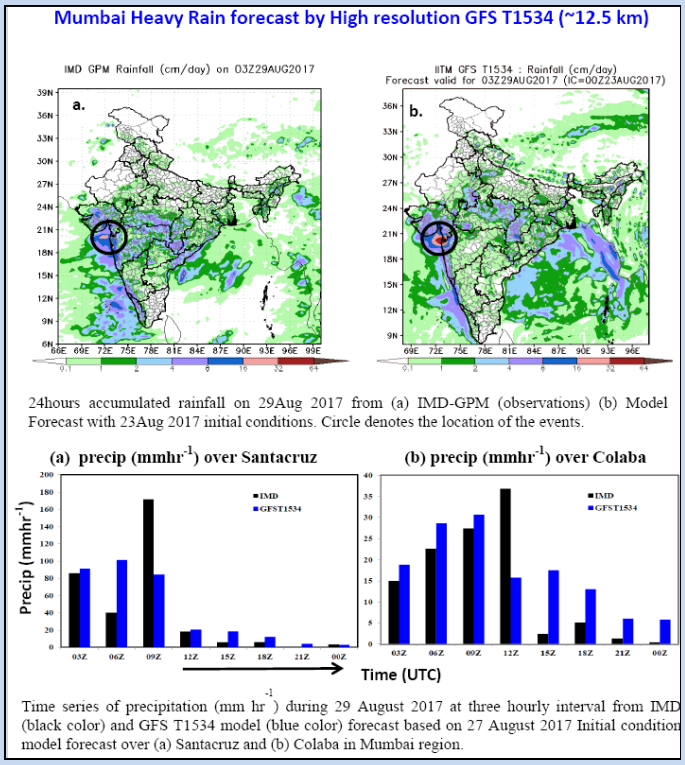

24hours accumulated rainfall on 29Aug 2017 from (a) IMD-GPM (observations) (b) Model Forecast with 23Aug 2017 initial conditions. Circle denotes the location of the events.

Time series of precipitation (mm hr^{-1}) during 29 August 2017 at three hourly interval from IMD (black color) and GFS T1534 model (blue color) forecast based on 27 August 2017 Initial condition model forecast over (a) Santacruz and (b) Colaba in Mumbai region.

P. Mukhopadhyay, V.S. Prasad, R. Phani Murali Krishna, Medha Deshpande, Malay Ganai, Snehlata Tirkey, Sahadat Sarkar, Tanmoy Goswami, C.J. Johny, Kumar Roy, M. Mahakur, V.R. Durai and **M. Rajeevan**

Indian Institute of Tropical Meteorology (IITM)
Earth System Science Organization (ESSO)
Ministry of Earth Sciences (MoES)
PUNE, INDIA
http://www.tropmet.res.in/

ISSN 0252-1075
Contribution from IITM
Research Report No. RR-146
ESSO/IITM/MM/SR/02(2019)/197

Performance of Very High Resolution Global Forecast System Model (GFS T1534) at 12.5km over Indian Region during 2016-2017 Monsoon Seasons

P. Mukhopadhyay*, V.S. Prasad, R. Phani Murali Krishna, Medha Deshpande, Malay Ganai, Snehlata Tirkey, Sahadat Sarkar, Tanmoy Goswami, C.J. Johny, Kumar Roy, M. Mahakur, V.R. Durai and **M. Rajeevan**

***Corresponding Author Address:**
Dr. P. Mukhopadhyay
Indian Institute of Tropical Meteorology,
Dr. Homi Bhabha Road, Pashan,
Pune – 411008, India.
E-mail: mpartha@tropmet.res.in; parthasarathi63@gmail.com
Phone: +91-(0)20-25904221

Indian Institute of Tropical Meteorology (IITM)
Earth System Science Organization (ESSO)
Ministry of Earth Sciences (MoES)
PUNE, INDIA
http://www.tropmet.res.in/

DOCUMENT CONTROL SHEET

Earth System Science Organization (ESSO)
Ministry of Earth Sciences (MoES)
Indian Institute of Tropical Meteorology (IITM)

ESSO Document Number
ESSO/IITM/MM/SR/02(2019)/197

Title of the Report
Performance of Very High Resolution Global Forecast System Model (GFS T1534) at 12.5km over Indian Region during 2016-2017 Monsoon Seasons

Authors
P. Mukhopadhyay*, V.S. Prasad, R. Phani Murali Krishna, Medha Deshpande, Malay Ganai, Snehlata Tirkey, Sahadat Sarkar, Tanmoy Goswami, C.J. Johny, Kumar Roy, M. Mahakur, V.R. Durai and M. Rajeevan

Type of Document
Scientific Report (Research Report)

Number of pages and figures
42, 18

Number of references
29

Keywords
Global forecast System (GFS) model, High resolution (12.5 km), Indian Monsoon

Security classification
Open

Distribution
Unrestricted

Date of Publication
June 2019

Abstract
GFS at horizontal resolution ~12.5 km is evaluated for the monsoon seasons of 2016-2017. Validation of rainfall for mean monsoon and individual months, indicates wet bias over the land region for all lead time. The PDF of forecast rainfall shows an overestimation (underestimation) for the moderate (0.25 – 1.56 cm day^{-1}) (heavy: 1.56-6.45 cm day^{-1}) categories. PDFs for extremely heavy rainfall (11.56 - 20.45 cm day^{-1}) are reasonable. The model reasonably predicts zonal wind at 850, 200 hPa, wind shear and vertical moisture profile. The diurnal rainfall phase and amplitude over most places is captured except the north-western part of India.

Summary

A very high resolution Atmospheric general Circulation Model (AGCM) Global Forecast System (GFS) model at horizontal resolution of 12.5 km (T1534) has been evaluated for the monsoon seasons (June-July-August-September) of 2016-2017. Although model shows awet bias over the land, the probability distribution (PDF) of rainfall shows better model fidelity in capturing the heavier rain categories (11.56-20.45 cm day^{-1}). The diurnal cycle has been forecast reasonably over Indian region except the north-western region. The diurnal cycle over oceanic region (equatorial Indian ocean, bay of Bengal and Arabian sea) has also been captured well by the model although it overestimates the amplitude. Establishment of GFS T1534 (12.5km) help to begin new initiatives such as the wind and solar renewable energy forecast. Use of GFS T 1534 as initial and boundary condition to dynamically downscale the forecast at turbine level is found to be skilful. Further research is initiated to improve model's physical parameterization which is suitable for higher spatial resolution.

Contents

Performance of very high resolution Global Forecast System Model (GFS T1534) at 12.5 km over Indian region during 2016-2017 monsoon seasons

P. Mukhopadhyay[1], V. S. Prasad[2], R. Phani Murali Krishna[1], Medha Deshpande[1], Malay Ganai[1], Snehlata Tirkey[1], Sahadat Sarkar[1], Tanmoy Goswami[1], C.J. Johny[2], Kumar Roy[1], M. Mahakur[1], V. R. Durai[3] and M. Rajeevan[4]

[1] Indian Institute of Tropical Meteorology, Dr. Homi Bhabha Road, Pashan, Pune-411008

[2.] National Centre for Medium Range Weather Forecasting, A-50, Sector-62, NOIDA, UP

[3.] India Meteorological Department, Mausam Bhavan, Lodi Road, New Delhi

[4.] Ministry of Earth Science, Government of India, Prithvi Bhavan, New Delhi

Corresponding Author

Dr. P. Mukhopadhyay
Indian Institute of Tropical Meteorology
Dr.HomiBhabha Road, Pashan, Pune 411008
Telephone: +91 20 25904221
FAX: +91 20 25865142
Email: mpartha@tropmet.res.in; parthasarathi63@gmail.com

Abstract

State of the art, atmospheric general circulation model (AGCM) Global Forecast System (GFS) at horizontal resolution of T1534 (~12.5 km) with 64 vertical levels have been evaluated here for the two monsoon seasons of 2016 and 2017. It is for the first time that such a high resolution model is being run operationally over the Indian region. It is therefore needed to have a detailed validation of the model during monsoon. Validation of mean monsoon rainfall for the June-July-August-September (JJAS) and the individual months indicate a tendency of wet bias of the model over the land region at all the forecast lead time. The probability distribution of forecast rainfall shows an overestimation of rainfall for the moderate categories (0.25 – 1.56 cm day^{-1}) and an underestimation of heavy rain categories of 1.56-6.45 cm day^{-1}. However forecast of extremely heavy rainfall PDFs (11.56 - 20.45 cm day^{-1}) are reasonable with respect to observation. The model shows reasonable prediction of large scale parameters associated with Indian summer monsoon e. g. zonal wind speed at 850 hPa (U850), zonal wind speed at 200 hPa (U200), easterly shear and most importantly the vertical profile of moisture in association with the regional Hadley cell and rainfall. Diurnal rainfall variability is always a challenge for the GCM. The diurnal analyses of GFS T1534 suggest, the model captures the diurnal phase and amplitude for all the lead time over most places of India except the north-west India. The diurnal cycle over the central India is found to be ahead of the diurnal peak time of observation. Although the model captures the diurnal cycle over the Bay of Bengal but shows an overestimation. It also overestimates the diurnal rainfall over the Western Ghats region. Over the equatorial Indian Ocean, model shows a reasonable diurnal cycle. Based on the skill scores of forecast, it is concluded that the model has a reasonable fidelity in capturing the spatio-temporal variability of monsoonal rain; however, further development is needed to enhance the skill of forecast for higher rain rate with longer lead.

1. Introduction

In the last several decades, there is a significant improvement in the skill of weather forecast using numerical weather prediction model. It is demonstrated globally that enhanced resolution of general circulation model improves the model fidelity. The increased skill of capturing variability has been aptly shown by Nonhydrostatic ICosahedral Atmospheric Model (Sato et al. 2005; Miura *et al.* 2015). Rajendran et al. (2008) have shown that the seasonal mean climate simulations have improved in high-resolution models. It is also reported that Community Atmosphere Model (CAM3) with higher resolution has shown improvement of simulation for the systems associated with large scale circulation (Hack et al. 2006). Williamson et al. (1995) showed that many nonlinear driving process of large scale circulation is represented better in high resolution models. Also European Center for Medium Range Weather Forecast (ECMWF) Integrated forecast system (IFS) model at 10 km resolution simulates the observed tropical cyclone frequency and intensity more reasonably than it's coarser resolution versions (Manganello et al. 2012).

In past, only few global centers explored General Circulation Models (GCM) for operational forecasting having resolution lesser than 100 km mainly due to limitation of computational resource. Recently, leading global operational centres e.g. ECMWF inducted very high resolution GCM for 10 days weather forecast. Many previous studies have reported the increasing tendencies of extreme events (Roxy et al. 2017; Goswami et al. 2006; Rajeevan et al. 2008) over the Indian region. Kim et al. (2018) highlighted the importance of the high resolution models to capture the extreme rainfall events over the Indian region. In India, the operational forecasting was based on the Global Forecast System (GFST574, Eulerian) model at 27 km resolution (Prasad et al. 2011) . Hence there was a need of high resolution particularly relevant for providing weather forecast at higher spatial resolution mainly for the extremes.

Currently NCMRWF GDAS provides the initial conditions for GFS T1534 model forecasts through hybrid 4D Ens-Var assimilation with T1534L64 (~12.5 km horizontal resolution) model resolution operationally since April 2017. However, in retrospect, routine generation of medium range forecasts started at NCMRWF in 1994 using T80L18 Global Data Assimilation and Forecasting (GDAF) system (Prasad et al. 2014). In course of time volume of data assimilated and model resolution increased considerably as a result of improvements in model, observing system and data reception system. Major improvement in forecasting skill was observed in 2010 with the introduction of T382L64 (~38 km horizontal resolution) model configuration and further up-gradation to T574L64 (~25 km horizontal resolution) in comparison with previous versions of model (Prasad et al. 2011). In 2011 monsoon period T574L64 model produced one day gain in forecast skill compared to T382L64 model (Prasad et al. 2014). In order to have a uniform data set (comparable skill) for a longer period that can be used for climate related studies, a retrospective analysis is carried out with model configuration of T574L64 from 2000 to 2011 (Prasad et al. 2017).

It is worthy to mention that since 2010 onwards, operational seasonal forecast based on the dynamical coupled model National Centre for Environmental Prediction (NCEP) CFSv2 (Climate Forecast System version 2 model) was used at T382 (~35km) resolution for Indian Summer Monsoon (ISM) forecast (June-July-August-September months) (Dandi et al. 2016). Along with the development of dynamical seasonal forecast model, an extended range multi-model (CFS/GFS) ensemble forecast system has also been developed to issue forecast up to 4 pentads. It is important to mention that Indian economy is largely dependent on agriculture (Gadgil and Gadgil 2006) vis-à-vis summer monsoon rainfall. The seasonal and extended range forecast system developed under “Monsoon Mission” of Ministry of Earth Science, Govt. of India, has been found to be very effective in enhancing the skill of forecast particularly for agricultural sector. Extended range forecast has also been found to be useful

for providing warnings of heat wave anomalies and extreme rainfall with 3 pentad lead times (Joseph et al. 2018; Borah et al. 2015).

While the seasonal forecast is able to provide skilful forecast of ISM over the country as a whole and the extended range forecast provides weekly anomalies over the region up to four pentads, hence there was an increasing demand particularly from the agro-met services to provide forecast advisories for a period of around 10 days at sub-district level. Increasing frequency of flood due to extreme rain (Nandargi and Gaur 2015) over the major Indian cities was a point of concern. Keeping particularly the requirement for a high resolution forecast over the country to enhance the services and extend it to sub-district level, a state of the art very high resolution NCEP GFS model (semi-Lagrangian) at T1534 (~12 km) has been established. In the present study, the evaluation of the high resolution model skill over the Indian region for two monsoon seasons (2016-2017) has been evaluated for the first time.

2. Model, Observation and Methodology

In order to fulfil the requirement for block level forecast in India, a very high resolution deterministic Global Forecast System (GFS) with spectral resolution of T1534 (~12.5 km) with 64 hybrid vertical levels (top layer around 0.27hPa) has been implemented for daily operational forecast since June 2016. The global atmospheric model in GFS is a global spectral model (GSM) version 13.0.2 adopted from NCEP (http://www.emc.ncep.noaa.gov/GFS/doc.php). The GFS model dynamical core is based on a two time-level semi-implicit semi-Lagrangian (SL) discretization approach (Sela 2010), while the physics is done in the linear, reduced Gaussian grid in the horizontal space. It is the first time that the SL dynamical core (previously Eulerian (EL)) is implemented in GFS T1534 for operational forecast over India equivalent to other global operational centers namely ARPEGE (Meteo France), GEM (Environment Canada), GFS (NCEP), GSM (JMA),

IFS (ECMWF), MetUM (UKMO) etc. The major advantage of SL framework over EL approach is that it is an unconditionally stable scheme which shows very good phase speeds and sufficient accuracy. It also saves lot of computational time as compared to EL framework due to longer time steps. A detailed description of the benefits of SL approach is described in detail in the study by Staniforth and Cote (1991). Figure 1 and Table 1 describe the schematic of GFS T1534 and description of model physics respectively. The initial conditions (ICs) for the forecast are generated by NCMRWF through the Global Data Assimilation System (GDAS) cycle which has more Indian data into it. More details about the NCMRWF data assimilation system is documented in Prasad et al. (2016).

The GFS T1534 model is run daily for 10 days and the output are stored at every 3 hour interval. In this report, we have analyzed both daily and diurnal runs of June-September (JJAS) for the years 2016 and 2017. The model is being run at IITM High Power Computer (HPC) "Aaditya".

To validate the model forecast, the latest version (05B) of Integrated Multi-satellite Retrievals for GPM (IMERG) (Huffman et al. 2014) rainfall data at 0.1°×0.1° (10 km) horizontal resolution and half hourly temporal resolution is used in the present study during JJAS of 2016 and 2017. The utilization of a very high resolution rainfall data is desirable to keep all the localized features intact in the observation and model. The precipitation in IMERG is estimated from various precipitation-relevant satellite passive microwave (PMW) sensors comprising the GPM constellation using the 2014 version of the Goddard Profiling Algorithm (GPROF2014). In the present study, we have used IMERG Version 05B final run data which is the latest high quality research purpose datasets and it is available in the following webpage https://pmm.nasa.gov/data-access/downloads/gpm. More technical details about the IMERG data sets are provided in

https://pmm.nasa.gov/sites/default/files/document_files/IMERG_doc_180207.pdf. For the present study we have interpolated the IMERG rainfall data from 0.1°×0.1° to 0.125°×0.125° model grid point.

In addition to rainfall data, various other satellite and reanalyses based parameters are also used to further investigate model performance. ERA Interim reanalysis (Dee et al. 2011) wind and relative humidity is utilized for the summer monsoon of 2016 and 2017. Additionally, the OLR data from Kalpana-1 very high resolution radiometer (VHRR) satellite observations (Mahakur et al. 2013) is used.

The daily rainfall time series is computed by accumulating half (three) hourly IMERG (GFS T1534) data. The model forecast data is taken from 22nd May of 2016 and 2017 respectively to make JJAS (122 days) time series at various lead time (Day-1 to Day-10) for both the year. The mean JJAS rainfall is calculated based on two year JJAS datasets for Day-1, Day-3, Day-5 and Day-8 forecast lead time. The spatial correlation coefficient is provided in the rainfall spatial plots. To make the diurnal cycle of rainfall over different parts of India, the 3 hourly time series is calculated for both observation and model starting from 0230IST to 2330 IST for various lead time.

3. Results and Discussion

3.1 Evaluation of rainfall and dynamical parameters

The forecasted rainfall with day-1, day-3, day-5 and day-8 lead for JJAS and the corresponding bias with respect to IMERG data are showed in Figure 2. While in all the lead times, the model prediction shows reasonable spatial correlation, there is a significant overestimation of rainfall over the Bay of Bengal region and over the west coast. The overestimation of the model forecast with respect to IMERG data, is evident in the precipitation bias plot as well (Figure 2). To understand the growth of bias, the rainfall bias

with different lead time for individual months of June, July, August and September are plotted in Figure 3. It is evident that the positive bias over the Bay region and along the west coast is present in all the months and at all the forecast lead time. This suggests that the model seems to have a systematic bias of overestimation over the Bay of Bengal and over the west coast region. The rainfall over the land also shows overestimation but lesser in magnitude as compared to that over the Bay of Bengal. The spatial correlation of model forecast precipitation with that of observation remains above 0.6 till 8 days during June and July. During August, the correlation falls to 0.62 to 0.52 from day 1 to day 8 lead time respectively. For the month of September, the model shows correlation upto 0.6 for forecast with 8 days (Figure 3) lead time. To identify the possible reason behind the model wet bias for different months and with different lead times, the rainfall probability distribution function (pdf) for all the months (JJAS) from the model forecast of day-1, day-3, day-5, day-8 and the corresponding observation is shown in Figure 4 (top left). The model overestimates the lighter rainfall (0.25 – 1.56 cm day^{-1}) at all the lead times, slightly underestimates the heavy rainfall categories (6.45-11.56 cm day^{-1}) and captures the very heavy categories (11.56-20.45 cm day^{-1}) for JJAS. To get further insight, model forecast in each month and for different lead time are analysed. Forecast rainfall pdf for the month of June and July appear to be reasonable for different categories. However, for August and September, forecast precipitation pdf shows overestimation for the lighter categories (0.25-1.56 cm day^{-1}) rain and underestimation in the heavy (6.45-11.56 cm day^{-1}) and very heavy categories (11.56-20.45 cm day^{-1}) rain.

As the pdf does not provide the spatial distribution of the rainfall, therefore to understand the spatial model performance for different rainfall categories, forecast rainfall for different categories are plotted in Figure5. It is evident from (Figure 5b-5e) that the model produces too much lighter rainfall over the Bay of Bengal, Western Ghats and also over the central

Indian region. While the model has a tendency to overestimate the lighter rains, the heavier rain categories are captured reasonably particularly over the Indian land mass.

The low level (850 hPa) and upper level (200 hPa) winds are found to be reasonably predicted although there is a slight overestimation of 850 hPa zonal wind around equatorial Indian ocean and of 200 hPa wind over the southern tip of Indian land mass (Figure 6). The easterly shear has been predicted well by the model (Figure 7). To identify the vertical distribution of moisture and the circulation (meridional-vertical), the regional Hadley cell (average over 65^{o}E-95^{o}E) is plotted for ERA and for day-1, day-3, day-5 and day-8 lead (Figure 8). In all the forecast lead, the model produces moderately (~65%) moist lower troposphere (within 850 hPa) and vertical extent of the moisture reaches upto 200 hPa before detraining in the upper troposphere. However, the model predicts a drier layers within 850 hPa to the north of 30N unlike the ERA reanalyses (Figure 8, top left). Higher moisture (~75%) in the lower tropospheric level (within 850 hPa) is seen only upto 10N in the model unlike the ERA analyses.

In order to gain more insight into the precipitation and moist processes over core central Indian region (18°N-27°N, 74°E-85°E), we have analyzed the vertical profile of relative humidity as a function of rain rate during JJAS, 2016-2017 (Figure 9). The similar metric has proven to be useful to look into the model moist dynamic processes (Abhik et al. 2017, Ganai et al. 2016). It is clear that for all the lead time that the model is able to capture the vertical pattern of relative humidity with corresponding rainfall threshold broadly. However, detailed analyses reveal that for all lead time model has systematically underestimated the lower level moisture distribution. Lower level moisture distribution plays an important role to trigger, sustain and to maintain growth of convective system. Thus, it may be possible that the

insufficient lower level moisture in model leads to make convection shallow which resulted in overestimation of lighter category rainfall and underestimation of heavier category rainfall. Another important aspect of the model is the diurnal rainfall variation namely the diurnal phase and diurnal absolute amplitude (Figure 10a-b). The definition of diurnal phase is that the local solar time (LST) whenthe maximum precipitation occurs in a day (Ganai et al. 2016). Diurnal absolute amplitude is defined as the difference between maximum rainfall and minimum rainfall in a day (Ganai et al. 2016). GFS T1534 captures the diurnal phase reasonably although except over the region of north-west India. For all the forecast lead times, the model captures the diurnal phase realistically elsewhere in the country. However, the absolute amplitude of the rain (Figure 10b) is overestimated over the Bay of Bengal and reasonable over the central Indian region. To further investigate the diurnal cycle of rainfall, we have selected eight boxes over different parts of Indian region as in Figure 11. Figure 12 shows the diurnal cycle of rainfall over different parts of India. Over the central Indian region, model captures a prominent variation but model peak rainfall is ahead of the observation. Over the Bay of Bengal model shows a similar rainfall variation as that of observation but with overestimation. Model fails to capture the rainfall variation over the north-west Indian region while over the north-east India, the model diurnal variation resembles the observation but with an overestimation. The diurnal rainfall variability over northern Western Ghats and southern Western Ghats appears to be overestimated in GFS T1534 as compared to IMERG. Further, the diurnal variation of rainfall is analysed over the western equatorial Indian ocean (WIO) and eastern equatorial Indian ocean (EIO) respectively. Although the EIO and WIO show weak diurnal variation, the model is able to capture the diurnal variation reasonably well over these two oceanic regions.

Above analyses bring out the fact that the model has the capability of capturing the diurnal cycle with reasonable fidelity but it has a tendency of overestimating the rainfall over the

western Ghats, Bay of Bengal and north-east India and does not match at north-west India. While the model predicts the heavier rainfall pdf well, it has the tendency of predicting too many lighter rainfall events over the Indian land mass and also over the Bay. These features of the model indicate the fact that model's cumulus and cloud parameterization, need further improvement to reduce frequent trigger of rain with moist PBL during the monsoon season. It may be worth mentioning that, although this model is being used at 12.5 km, but most of the physical parameterization particularly the cloud and convective parameterization of GFS is same as that of the coarser resolution GFS/CFS. Such tendency of overestimation of lighter rain in rainfall pdf was earlier reported by Goswami et al. (2014), Abhik et al. (2016) in analysing CFSv2T126 and CFSv2T382 respectively. Thus, while the model has good fidelity of capturing the diurnal cycle over the land and ocean and also capable of capturing the heavier rainfall pdf, there is a need to improve the physics suitable with the higher resolution (~12.5km) of the model and subsequent modification of convective trigger that will reduce the generation of too frequent lighter rain and may improve the model bias. Another aspect which may be needed to be improved is the vertical resolution of the GFS T1534. The CFSv2 T126, CFSv2T382, GFST574 and this version GFS T1534 all use 64 vertical levels, while with the increase of horizontal resolution, there is a need to enhance the vertical resolution as well for resolving the vertical processes associated with the cloud and convection of the model.

3.2 Verification of model forecast

To further assess the performance of GFS T1534 quantitatively, skill scores of rainfall over Indian land points are calculated. The forecast skill of GFS T1534 (JJAS of 2016-2017) is assessed based on skill scores such as Equitable Threat Score (ETS), Peirce Skill Score (PSS), Heidke Skill score (HSS) and so on. These scores provide quantitative information of the fidelity of model forecast with respect to observation. The dichotomous nature of

precipitation allows for verification using contingency table. The contingency table is shown in Table 2. This has four components namely hits, ‘a’, false alarms, ‘b’, miss, ‘c’ and correct negatives ‘d’. Skill scores are based on these components.

Table 2: Structure of the contingency table (Finley 1884)

		Observed (o)		**Total**
		Yes	**No**	
Forecast (f)	**Yes**	*Hits* ***a***	*False alarms* ***b***	*Forecast yes* ***a+b***
	No	*Misses* ***c***	*Correct negatives* ***d***	*Forecast no* ***c+d***
Total		*Observed Yes* ***a+c***	*Observed no* ***b+d***	*Total* ***N= a+b+c+d***

Here we have calculated the ETS,PSS and HSS to assess the skill of GFS T1534. ETS gives the indication as to how well the forecast yes events corresponds to observed yes events accounting for hits which might occur by chance. This score ranges from -1/3 to 1 with 1 being the perfect score. It is given by

$$ETS = \frac{a - a_{ref}}{a+b+c-a_{ref}} \qquad (1)$$

Where, $a_{ref} = \frac{(a+b)(a+c)}{a+b+c+d}$ (1a)

PSS tells how well the forecast could distinguish between ‘yes’ events from ‘no’ events. It is the difference between probability of detection and probability of false detection. The score ranges from -1 to 1 with 1 being the perfect score. It is given by,

$$PSS = H - F = \frac{ad-bc}{(a+c)(b+d)} \qquad (2)$$

Heidke Skill Score shows the accuracy of forecast relative to that of random chance. It ranges from -1 to 1 with 0 showing no skill and 1 being perfect score.

$$HSS = \frac{2(ad-bc)}{(a+c)(c+d)+(a+b)(b+d)} \qquad (3)$$

Figure 13a-c shows the ETS, PSS and HSS for GFS T1534 with increasing threshold and lead time respectively. ETS attains a maximum score of 0.26 for Day 1, PSS attains a maximum score of 0.43 for Day 1 and HSS peaks at 0.41 for Day 1. The scores decrease with increasing lead time and thresholds. Here it is worthwhile to note that the scores do not fall to zero even for threshold as high as 105 mm and lead time of Day 5. This indicates reasonably good forecast skill of the model. Comparison of earlier versions of GFS (e. g. GFS T382, T574 etc.) were compared by Prasad et al. (2014) and Singh and Prasad (2018) which establish the better skill of GFS T1534 as compared to earlier version of the model.

Another set of scores is shown in the performance diagram which comprises of Probability of Detection (POD), Success Ratio (SR), Bias Score (B) and Critical Success Index (CSI). This was devised by Roebber 2009, details can be found therein. The scores are calculated based on contingency table and expressed as,

$$POD = \frac{a}{a+c} \quad (4)$$

$$SR = 1 - False\ Alarm\ Ratio = \frac{a}{a+b} \quad (5)$$

$$B = \frac{a+b}{a+c} \quad (6)$$

$$CSI = \frac{a}{a+b+c} \quad (7)$$

Figure 14 shows the performance diagram of GFS T1534 for Day 1, 3 and 5 and for thresholds of 2.5, 5, 15 and 20 mm. The X and Y axis show Success Ratio and Probability of Detection respectively. The dashed and curved lines represent Bias and Critical Success Index respectively. Perfect value for all these scores is 1 hence in the diagram a good forecast

will lay in the top right quadrant aligned to the 45˚ diagonal. Here we can clearly see that the skill of forecast decreases with increasing lead times. Also for a particular lead time, the skill decreases with increasing threshold. Although it is noteworthy that Bias is improving with increasing lead time.

Further, verification of wind forecast is carried out in terms of Root Mean Square Error (RMSE). RMSE is calculated for u (Figure 15a) and v (Figure 15b) components of wind at 850 hPa and 200 hPa for the ISM domain (10˚S-40˚N, 50˚E-120˚E). For both the components of winds, there is gradual increase in RMSE with lead time. RMSE is less for v compared to u component at 850 hPa and 200 hPa. A point of note is that the error for u and v at 850 hPa is considerably less than at 200 hPa. Even at Day 5 RMSE lies below 6 m/s for both the cases which indicates good skill of the model in predicting winds.

4. Applications of GFS T1534 forecast

4.1 Forecasting of Wind and Solar renewable energy with GFS T1534 as Initial Conditions

IITM has taken initiative to forecast wind and solar energy using high-resolution regional models (WRF-ARW and WRF-SOLAR). These models are initialized using GFST1534 initial condition and they are run over the specific site over Maharashtra State with 1 km horizontal resolution and a day ahead (~48hrs) forecast is generated with every 15 min interval. The model is run for JJAS-2016, July 2017 as well as many individual cases and validated with station level data obtained from a solar and wind generator's site at Maharashtra. Different experiments are also conducted with the land use and land cover (LU/LC) data from ISRO. The model's performance is improved with the bias correction method. The skill based on an average MNRE's percentage error lies below 1% and hardly crosses 3%. The further developmental work is under progress.

4.2 Prediction of heavy rainfall events

The forecast from GFS T1534 can be used for prediction of heavy rainfall events 4-5 days in advance .

Mumbai (29 Aug. 2017) event: The observed 12 hours accumulated rainfall for Mumbai was 468 cm. From the spatial pattern of rainfall (Figure 17), it is clear that model was able to predict the event 5-days in advance. Three hourly variation of rainfall on 29 Aug 2017 is well captured by the model with two days lead (Figure 18).

4.3 Forest fire monitoring

The 10 days forecast output of GFS T1534 (12km) has been shared with Forest Survey of India, Ministry of Environment, Forest and Climate-change. With the dry (moist) environment and high (low) winds, the probability of forest fire is higher (lesser). The surface winds and the humidity forecast provided from GFS T1534 are used as initial conditions in the statistical fire model which is further used for forecasting the forest fire one week in advance.

5. Conclusions

The deterministic forecast from the high resolution GFS T1534 (12km) model has been evaluated for two monsoon seasons e. g. 2016 and 2017. The model being initialised with the GDAS assimilation at NCMRWF, is run every day for next 10 days forecast at IITM. The evaluation of the high resolution model forecast reveals that the model broadly is able to capture the heavy rainfall PDFs although it has the systematic error of producing more than observed lighter and moderate categories of rain rates. The tendency of overestimating lighter and moderate rain rates is evident in the spatial plots and for all the lead times of the forecast. Critical evaluation of moisture distribution reveals that the model is able to capture the

vertical structure associated with the regional Hadley cell reasonably although the low level moisture maximum extends up to around 10˚N as against ERA reanalyses where the maximum moisture within boundary layer extends up to 20˚N. The model shows a good fidelity in forecasting the diurnal phase over the country except over the north-west region. The diurnal cycle over the central India region needs further improvement in terms of time of peak rain. The diurnal rainfall over the Western Ghats, Bay of Bengal and the north-eastern region needs to be further improved to reduce the overestimation.

The model shows reasonable skill for various rainfall categories although the skill reduces with the lead time. While the model shows fidelity in capturing the lower (850 hPa) and upper (200 hPa) level wind and moisture distribution with reasonable accuracy, there is a need to enhance the skill for higher categories of rain rates with longer lead. Further model development in improving the model dynamical core from Gaussian linear to cubic spectral octahedral grid, incorporating improved convection and better microphysics etc. initiatives are being undertaken in improving the model performance with reduced forecast error.

Acknowledgements

IITM is an autonomous research Institution, fully supported by the Ministry of Earth Sciences (MoES), Govt. of India, New Delhi. The GFS model is run on "Aaditya" MoES High Power Computing system located at IITM, Pune. Authors thank IMD for TRMM and Rain gauge merged daily rainfall data. RPMK gratefully acknowledges and thank Dr. S Moorthi, National Center for Environmental Prediction, USA for the help in understanding the Semi-Lagrangian framework. Authors from IITM, Pune are grateful to Director, IITM for encouragement and support.

References

Abhik S, Mukhopadhyay P, Krishna RPM, Salunke KD, DhakateAR and Rao SA (2016) Diagnosis of boreal summer intraseasonal oscillation in high resolution NCEP climate forecast system. *Climate dynamics*, **46(9-10)**, pp.3287-3303.

Abhik S, Krishna RP M, Mahakur M, Ganai M, Mukhopadhyay P and Dudhia J (2017) Revised cloud processes to improve the mean and intraseasonal variability of Indian summer monsoon in climate forecast system: Part 1. *Journal of Advances in Modeling Earth Systems*, **9(2)**, pp.1002-1029.

Borah N, Sahai A K, Abhilash S, Chattopadhyay R, Joseph S, Sharmila S and Kumar A (2015) An assessment of real-time extended range forecast of 2013 Indian summer monsoon; *Int. J. Climatol*., **35**, 2860–2876

Dandi A R, Sabeerali C T, Chattopadhyay R, Rao D N, George G, Dhakate A, Salunke K, Srivastava A and Rao A S (2016) Indian summer monsoon rainfall simulation and prediction skill in the CFSv2 coupled model: Impact of atmospheric horizontal resolution; *J. Geo. Phy. Res. Atmos*., **121(5)**, 2205-2221

Dee D P, Uppala S M, Simmons A J, Berrisford P, Poli P, Kobayashi S, Andrae U, Balmaseda M A, Balsamo G, Bauer P, Bechtold P, Beljaars A C M, van de Berg L, Bidlot J, Bormann N, Delsol C, Dragani R, Fuentes M, Geer A J, Haimberger L, Healy S B, Hersbach H, Hólm E V, Isaksen L, Kållberg P, Köhler M, Matricardi M, McNally A P, Monge-Sanz B M, Morcrette J.-J, Park B.-K, Peubey C, de Rosnay P, Tavolato C, Thépaut J.-N and Vitart F (2011) The ERA-Interim reanalysis: configuration and performance of the data assimilation system. *Q.J.R. Meteorol. Soc*., **137**: 553–597. doi: 10.1002/qj.828 Finley J.P, 1884: Tornado predictions. *Amer. Meteor*. J., **1**, 85-88

Gadgil S and Gadgil S (2006) The Indian monsoon, GDP and agriculture; *Econ. Polit. Wkly*., **41**, 4887–4895

Ganai M, Krishna R P M, Mukhopadhyay P and Mahakur M (2016) The impact of revised simplified Arakawa-Schubert scheme on the simulation of mean and diurnal variability associated with active and break phases of Indian summer monsoon using CFSv2. *Journal of Geophysical Research: Atmospheres*, **121(16)**, pp.9301-9323.

Goswami BN, Venugopal V, Sengupta D, Madhusoodanan MS and Xavier PK (2006) Increasing trend of extreme rain events over India in a warming environment, *Science*, **314(5804)**, pp.1442-1445.

Hack J J, Caron J M, Danabasoglu G, Oleson K W, Bitz C and Truesdale J (2006) CCSM–CAM3 climate simulation sensitivity to changes in horizontal resolution. *J. Clim*, **19**, 2267–2289

Huffman G, Bolvin D, Braithwaite D, Hsu K, Joyce R, Xie P (2014) Integrated Multi-satellite Retrievals for GPM (IMERG), version 4.4. NASA's Precipitation Processing Center, accessed 31 March, 2015, ftp://arthurhou.pps.eosdis.nasa.gov/gpmdata/

Joseph S, Mandal R, Sahai A K, Phani R, Dey A and Chattopadhyay R (2018): Diagnostics and Real –Time Extended Range Prediction of Heat Waves over India; IITM research report (ISSN 0252-1075), ESSO/ IITM/SERP/ SR/03(2018)/192

Kim IW, Oh J, Woo S and Kripalani R H (2018) Evaluation of precipitation extremes over the Asian domain: observation and modelling studies. *Clim. Dyn.*, pp.1-26. https://doi.org/10.1007/s00382-018-4193-4

Mahakur M, Prabhu A, Sharma AK, Rao VR, Senroy S, Singh R, Goswami BN (2013) High-resolution outgoing longwave radiation dataset from Kalpana-1 satellite during 2004–2012. *Curr Sci.***105**:1124–1133

Manganello J V, Hodge K I, Kinter J L and others (2012) Tropical Cyclone Climatology in a 10-km Global Atmospheric GCM:Toward Weather-Resolving Climate Modeling; *J. Clim.*, **25**, 3867-3893.

Miura H, Suematsu T and Nasuno T (2015) An ensemble hindcast of the Madden-Julian Oscillation during the CINDY2011/DYNAMO field campaign and influence of seasonal variation of sea surface temperature; *J. Meteor. Soc. Japan*, **93A**, 115-137

Nandargi S S and Gaur A (2015) Extreme Rainfall Events over the Uttarakhand State (1901-2013); *Int. Journal of Sci. and Res*., **4(4)**, 700-703

Prasad V S, Saji Mohandas, Munmun Das Gupta, Rajagopal E N and Surya KantiDatta (2011) Implementation of upgraded Global Forecasting Systems (T382L64 and T574L64) at NCMRWF, NCMRWF Technical Report No. NCMR/TR/5/2011 May 2011, 72p, http://www.ncmrwf.gov.in/ncmrwf/gfs report final.pdf.

Prasad V S, Mohandas S, Dutta S K, Das Gupta M, IyengarG R, Rajagopal E N and Basu S (2014) Improvements in medium range weather forecasting system of India. *J. Earth Syst. Sci*., **123(2)**, 247–258.

Prasad V S, Johny CJ and Sodhi J S (2016) Impact of 3D Var GSI-ENKF hybriddata assimilation system.*J. Earth Syst. Sci.*, **125(8)**, pp. 1509-1521.

Prasad V S, Johny C J, Mali P, Singh S K, and Rajagopal E N (2017) Retrospective Analysis of NGFS for the years 2000-2011. *Curr Sci*., **112**, 2, 370-377.

Rajeevan M, Bhate J and Jaswal A K (2008) Analysis of variability and trends of extreme rainfall events over India using 104 years of gridded daily rainfall data. *Geophysical Research Letters*, **35(18)**.

Rajendran K and Kitoh A (2008) Indian summer monsoon in future climate projection by a super high-resolution global model. *Curr Sci.*, pp.1560-1569.

Roebber, P. J. (2009). Visualizing multiple measures of forecast quality. *Weather and Forecasting*, **24(2)**, 601-608.

Roxy M K, Ghosh S, Pathak A, Athulya R, Mujumdar M, Murtugudde R, Terray P and Rajeevan M (2017) A threefold rise in widespread extreme rain events over central India. *Nature Communications*, ***8*(1)**, p.708.

Sato M, Tomita H, Miura H, Iga S and Nasuno T (2005) Development of a global cloud resolving model-a multi-scale structure of tropical convections; *J. of the Earth Simulator*, **3**, 11 – 19

Sela J (2010): The derivation of sigma pressure hybrid coordinate semi-Lagrangian model equations for the GFS. NCEP Office Note 462 pp31.

Sanjeev Kumar Singh, and V. S. Prasad, 2018: Evaluation of precipitation forecasts from 3-D Var and Hybrid GSI-Based system during Indian summer monsoon 2015. Meteorology and Atmospheric Physics, doi: 10.1007/s00703-018-0580-y.

Staniforth A. and Cˆot´e J. (1991). Semi-Lagrangian integration schemes for atmospheric models – a review. *Mon. Weather Rev*. **119**, 2206–2223.

Williamson D L, Kiehl J T and Hack J J (1995) Climate sensitivity of the NCAR Community Climate Model (CCM2) to horizontal resolution. *Clim. Dyn*., **11**, 377 – 397

Figure captions

Figure 1.Schematic of GFS T1534

Table 1.*Model physics in GFS T1534*

Table 2:*Structure of the contingency table (Finley 1884)*

Figure 2.JJAS mean rainfall (mm/day) for Day-1, Day-3, Day-5 and Day-8 lead time form GFS T1534 model forecast and compared with IMERG gridded data. Spatial pattern correlation coefficients between model and observation at different lead time over Indian land points. Right hand column represents model rainfall (mm/day) bias at various lead time with respect to observation.

Figure 3.JJAS rainfall bias (mm/day) for Day-1, Day-3, Day-5 and Day-8 lead time form GFS T1534 model forecast with respect to IMERG gridded data.

Figure 4.All India rainfall PDF (%) versus rain rate (cm/day) categories during JJAS, June, July, August and September respectively for different lead time derived from GFS T1534 model forecast and compared with IMERG gridded data.

Figure 5.Spatial distribution of rainfall (cm/day) for different categories during JJAS for (a) IMERG and (b-e) GFS T1534 for different lead time.

Figure 6. Spatial distribution of zonal wind circulation bias (m/s) in GFS T1534 with respect to ERA Interim at Day-1, Day-3, Day-5 and Day-8 lead time at 850hPa (left side two column) and 200hPa (right side two column).

Figure 7. Easterly zonal wind shear (m/s) (U200-U850) during JJAS over Indian region as obtained from ERA Interim and GFS T1534 at various lead time.

Figure 8. Regional Hadley circulation (vector in m/s) and Relative humidity (shaded in %) distribution over Indian summer monsoon domain during JJAS as obtained from ERA Interim (top left figure) and GFS T1534 model forecast at different lead time respectively.

Figure 9. Vertical profile of relative humidity (shaded in %) as a function of rain rate (mm/day) over central Indian region during JJAS of 2016-2017 from observation (ERA-Interim versus IMERG, top left side) and GFS T1534 at various lead timerespectively. The rain rate at the x axis is plotted in log10 scale.

List of Tables

Table 1. *Model physics in GFS T1534*

Physics	Description
Convection	Revised Simplified Arakawa-Schubert (RSAS) and mass flux based SAS shallow convection scheme
Microphysics	Zhao-Carr-Moorthi microphysics formulation for grid-scale condensation and precipitation
Gravity Wave Drag	Orographic gravity wave drag, mountain-drag and stationary convective gravity wave drag
PBL	Hybrid Eddy Diffusion Mass flux turbulence/vertical diffusion scheme
Radiation	Solar radiation and IR based on RRTM (originally from AER, modified at EMC) with Monte Carlo Independent Column Approximation (McICA). Cloud fraction for radiation computed diagnostically from prognostic cloud condensate

Table 2: *Structure of the contingency table (Finley 1884) [after fig. 17]*

		Observed (o)		**Total**
		Yes	**No**	
Forecast (f)	**Yes**	*Hits* ***a***	*False alarms* ***B***	*Forecast yes* ***a+b***
	No	*Misses* ***c***	*Correct negatives* ***d***	*Forecast no* ***c+d***
Total		*Observed Yes* ***a+c***	*Observed no* ***b+d***	*Total* ***N= a+b+c+d***

Table 3: *Abbreviation used in the report*

Abbreviation	Full expression
AGCM	Atmospheric General Circulation Model
GFS	Global Forecast System
CAM	Community Atmospheric Model
GCM	General Circulation Model
ECMWF	European Centre for Medium range Weather Forecast
IFS	Integrated Forecast System
NCEP	National Centre for Environmental Prediction
GPM	Global Precipitation Measurement
IMERG	Integrated Multi-satellite Retrievals for GPM
ARPEGE (Meteo France),	Action de Recherche Petite Echelle Grande Echelle
GEM (Environment Canada)	Global Environmental Multiscale Model

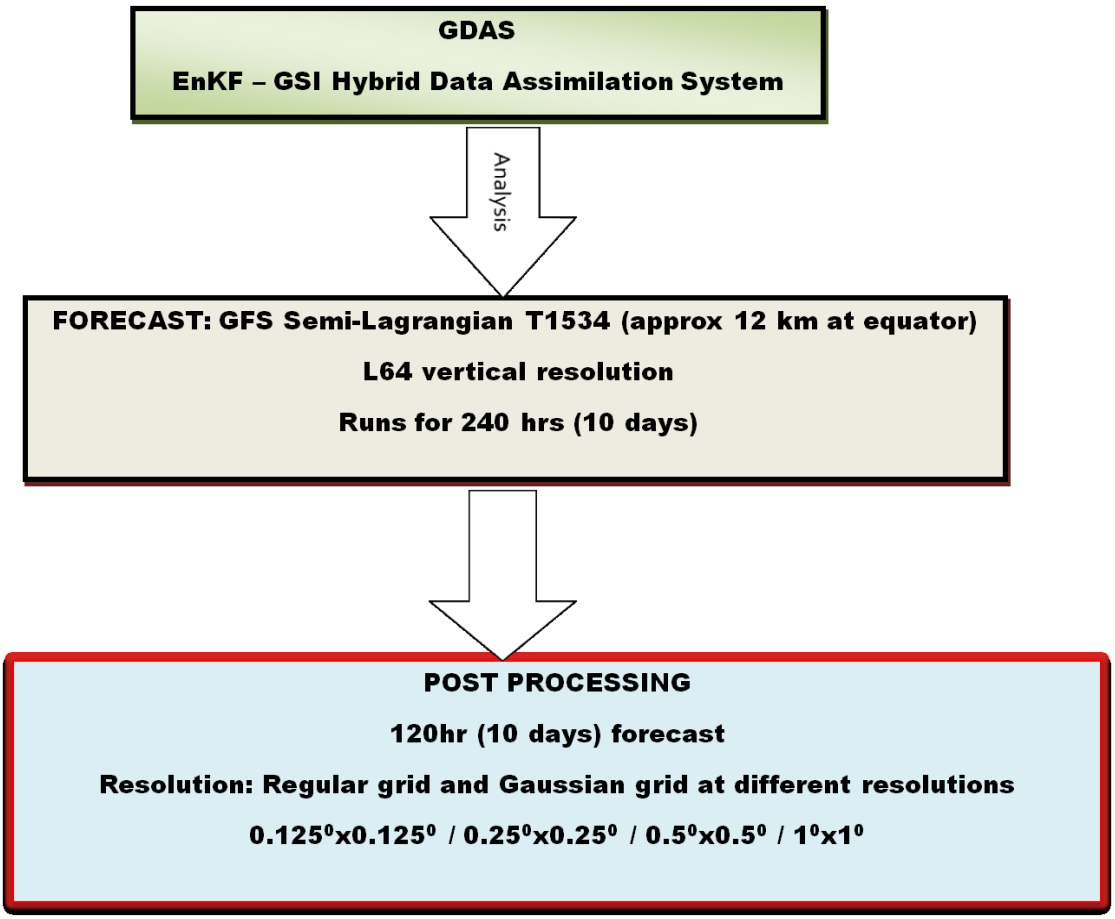

Figure 1. Schematic of GFS T1534

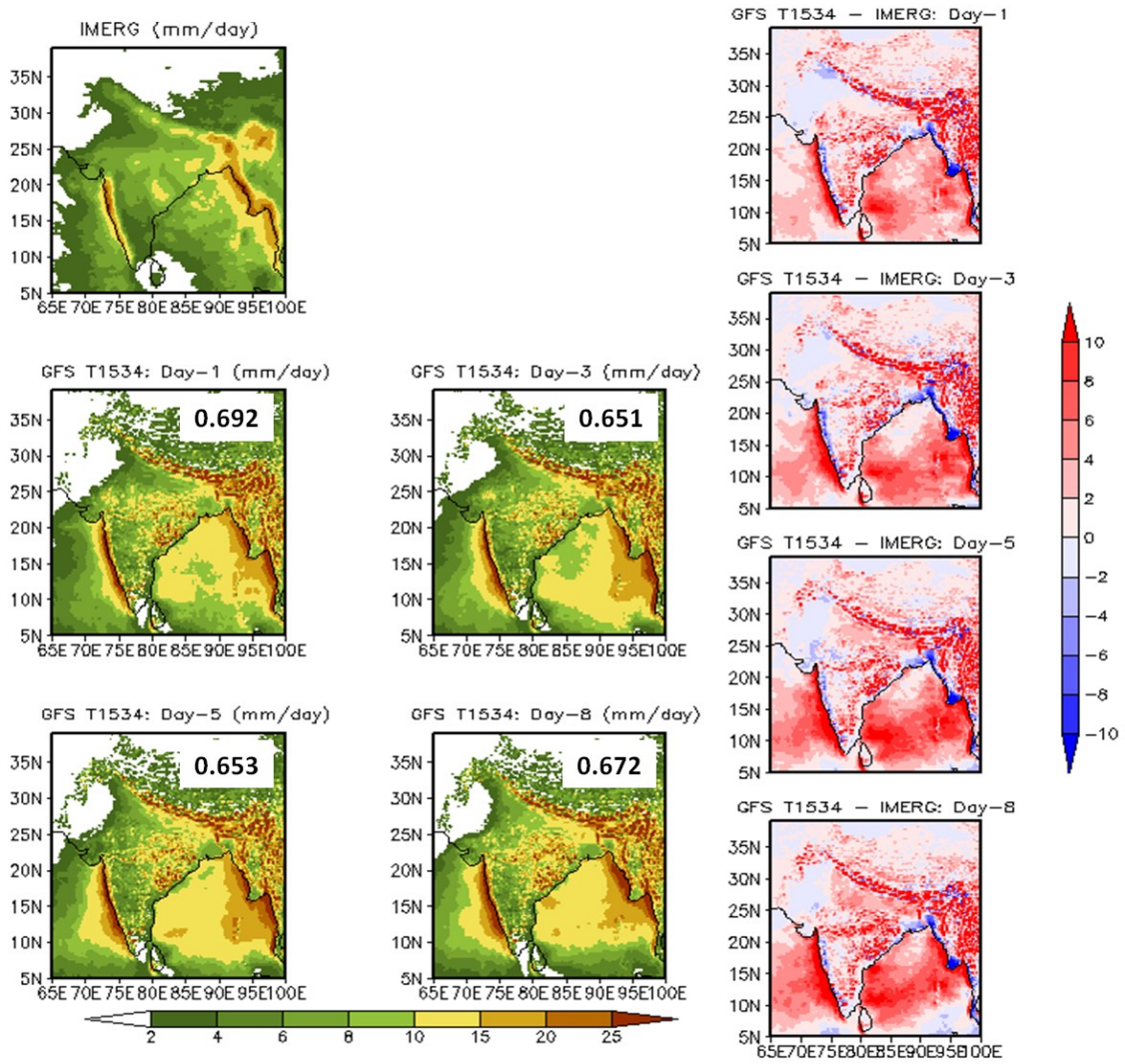

Figure 2: JJAS mean rainfall (mm/day) for Day-1, Day-3, Day-5 and Day-8 lead time form GFS T1534 model forecast and compared with IMERG gridded data. Spatial correlation coefficients between model and observation at different lead time. Right hand column represents model rainfall (mm/day) bias at various lead time with respect to observation.

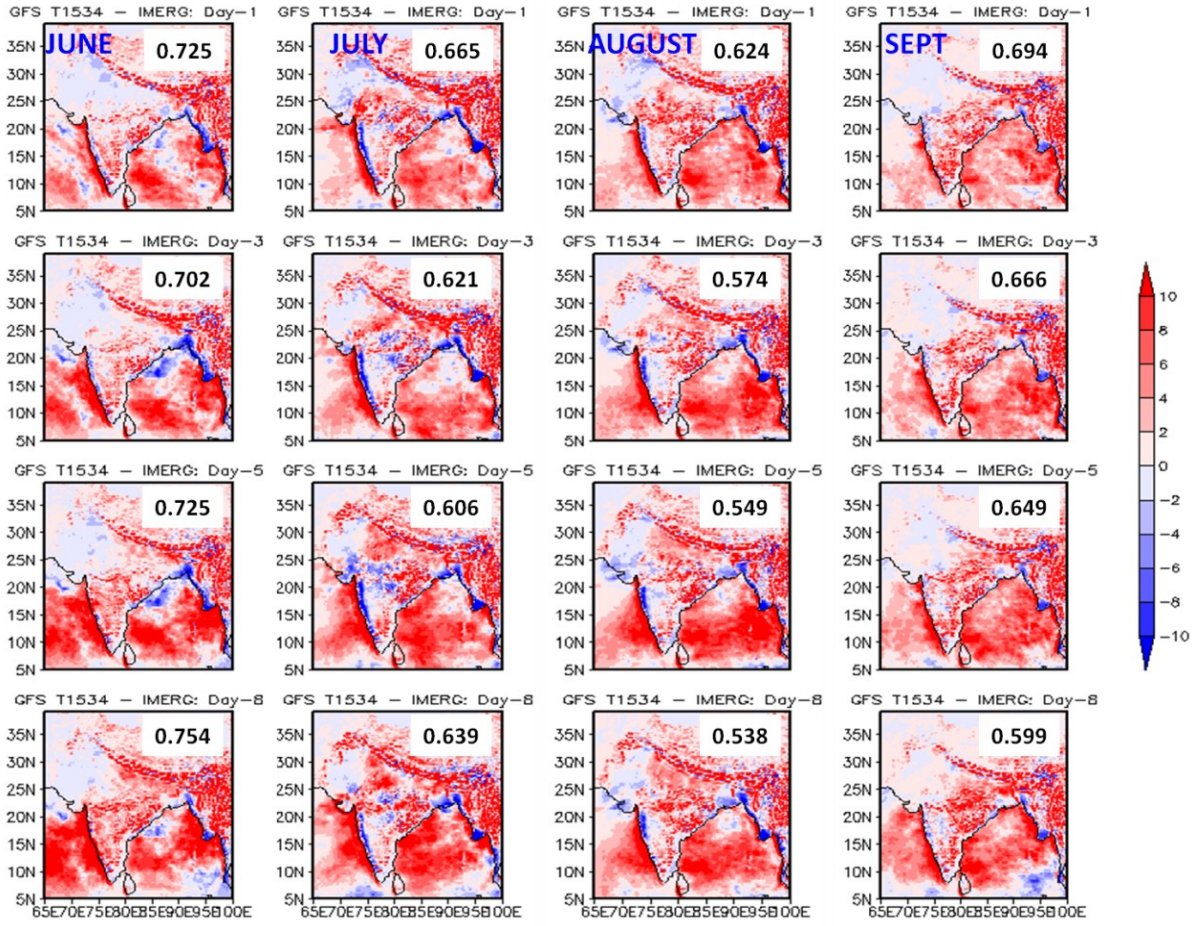

Figure 3. Rainfall bias (mm/day) for Day-1, Day-3, Day-5 and Day-8 lead time form GFS T1534 model forecast with respect to IMERG gridded data during June, July, August and September respectively.

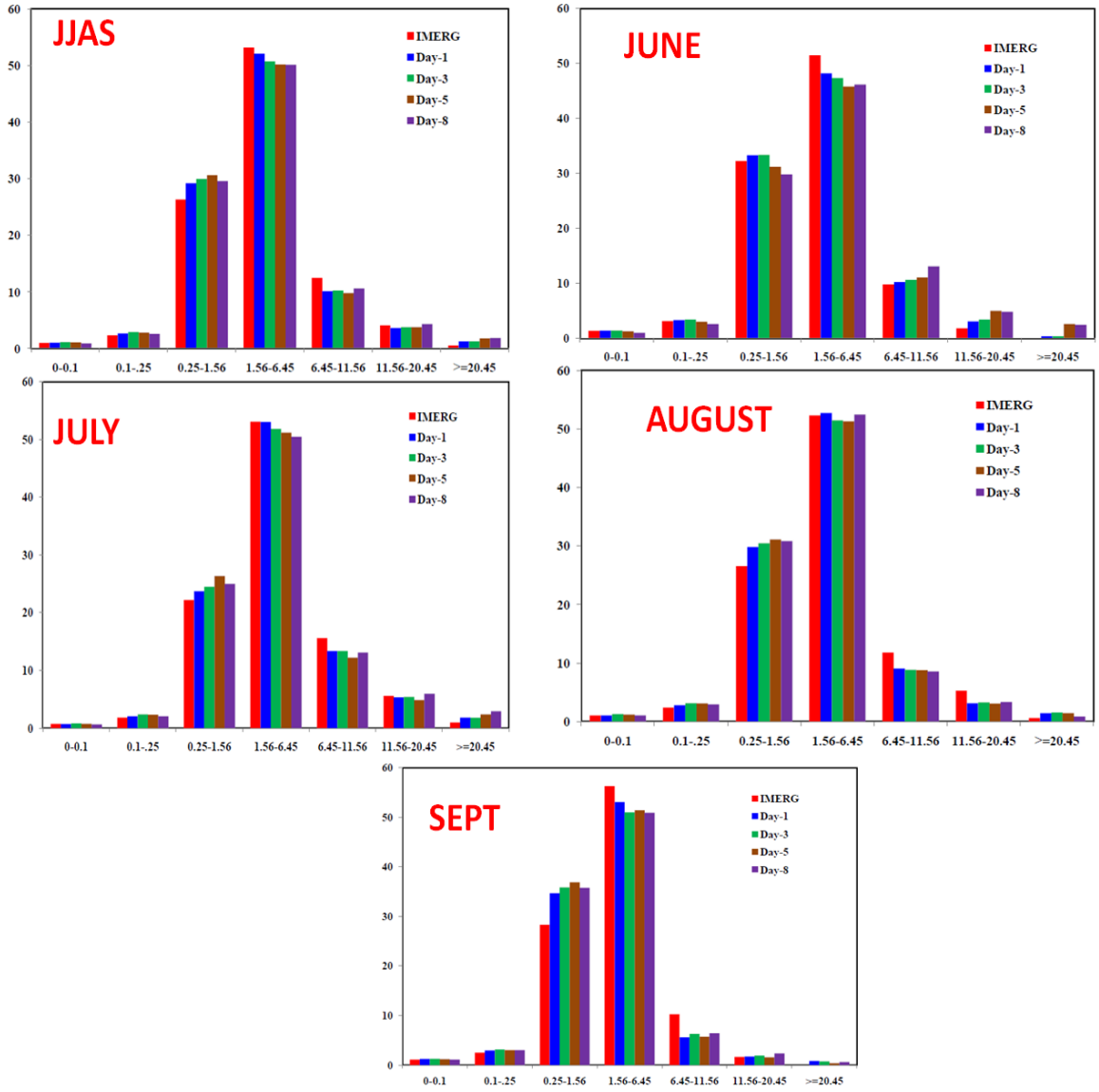

Figure 4. All India rainfall PDF (%) versus rain rate (cm/day) categories during JJAS, June, July, August and September respectively for different lead time derived from GFS T1534 model forecast and compared with IMERG gridded data.

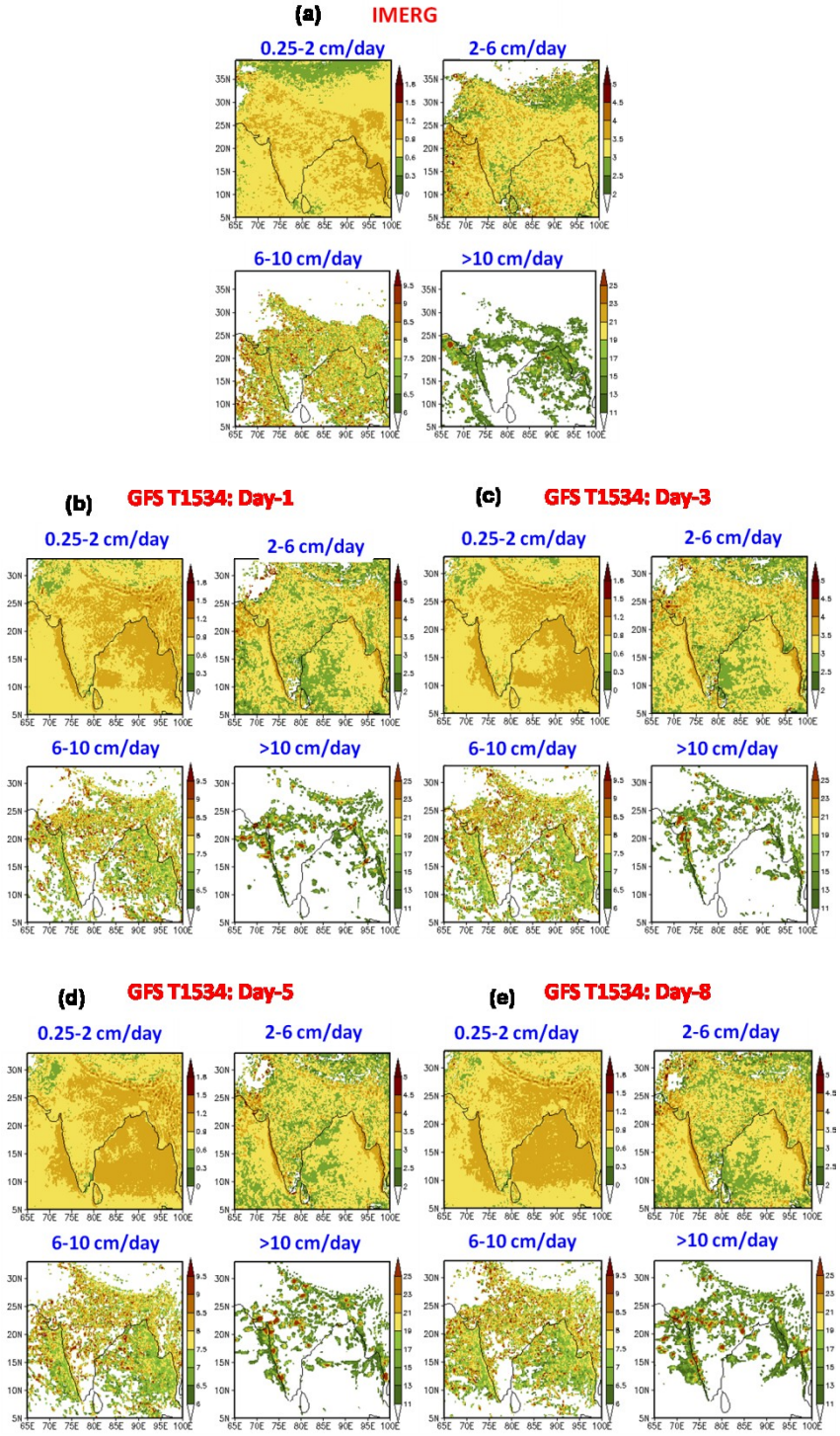

Figure 5. Spatial distribution of rainfall (cm/day) for different categories during JJAS for (a) IMERG and (b-e) GFS T1534 for different lead time.

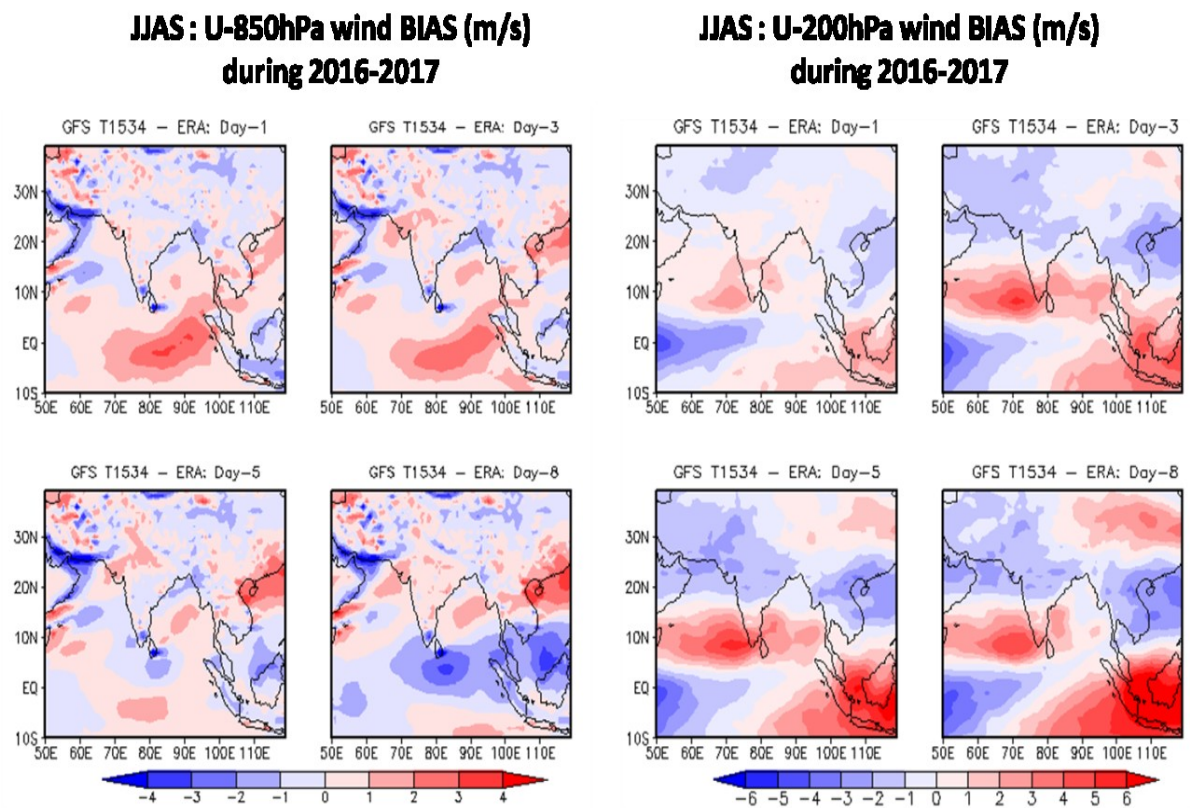

Figure 6. Spatial distribution of zonal wind circulation bias (m/s) in GFS T1534 with respect to ERA Interim at Day-1, Day-3, Day-5 and Day-8 lead time at 850hPa (left side two column) and 200hPa (right side two column).

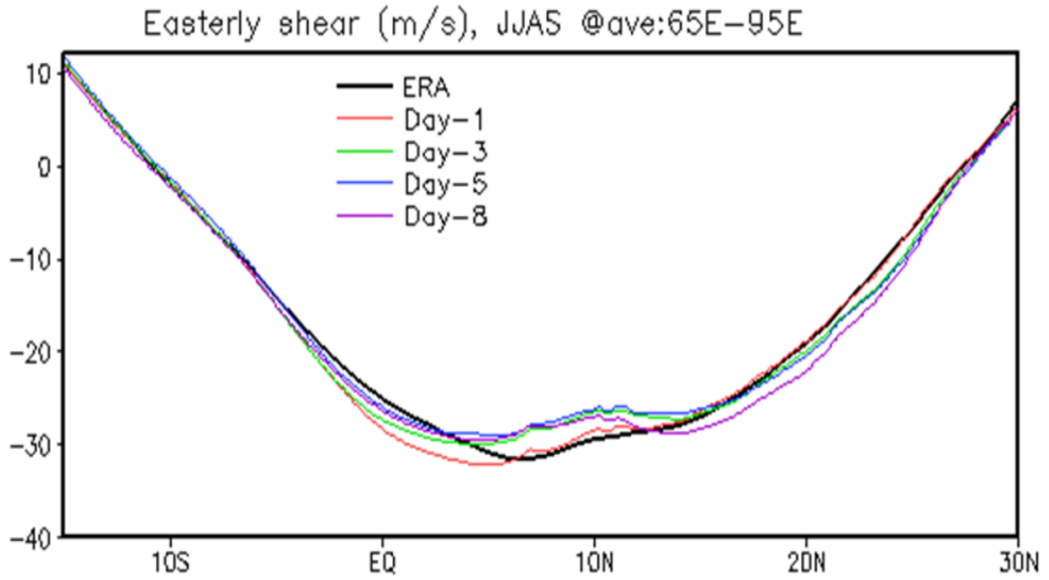

Figure 7. Easterly zonal wind shear (m/s) (U200-U850) during JJAS over Indian region as obtained from ERA Interim and GFS T1534 at various lead time.

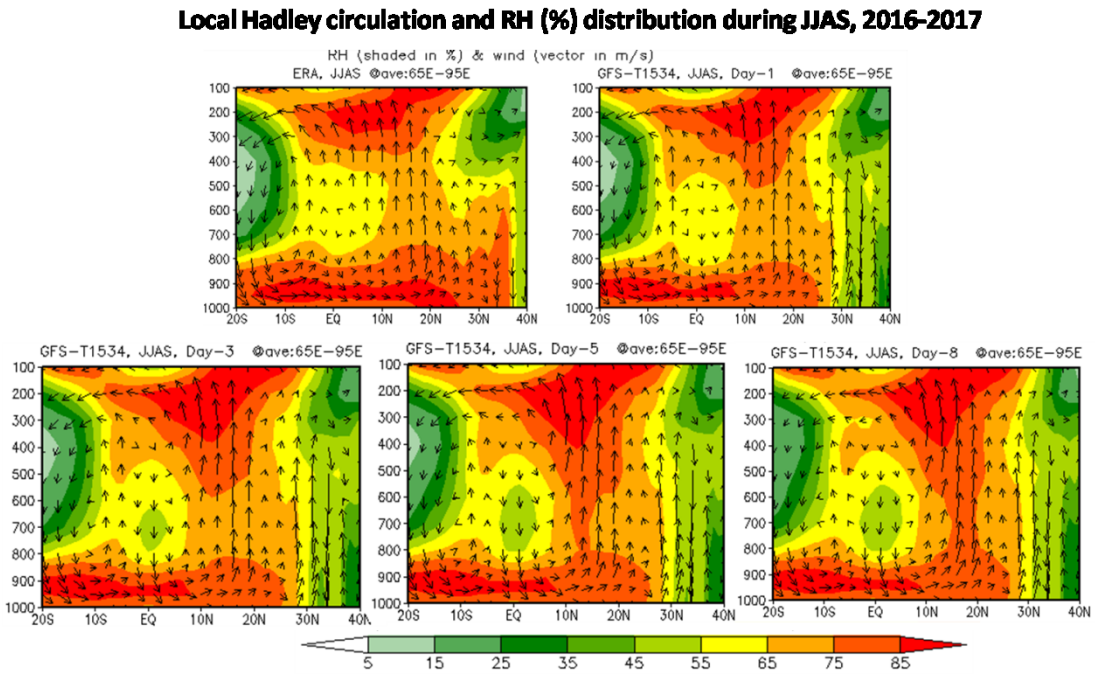

Figure 8. Regional Hadley circulation (vector in m/s) and Relative humidity (shaded in %) distribution over Indian summer monsoon domain during JJAS as obtained from ERA Interim (top left figure) and GFS T1534 model forecast at different lead time respectively.

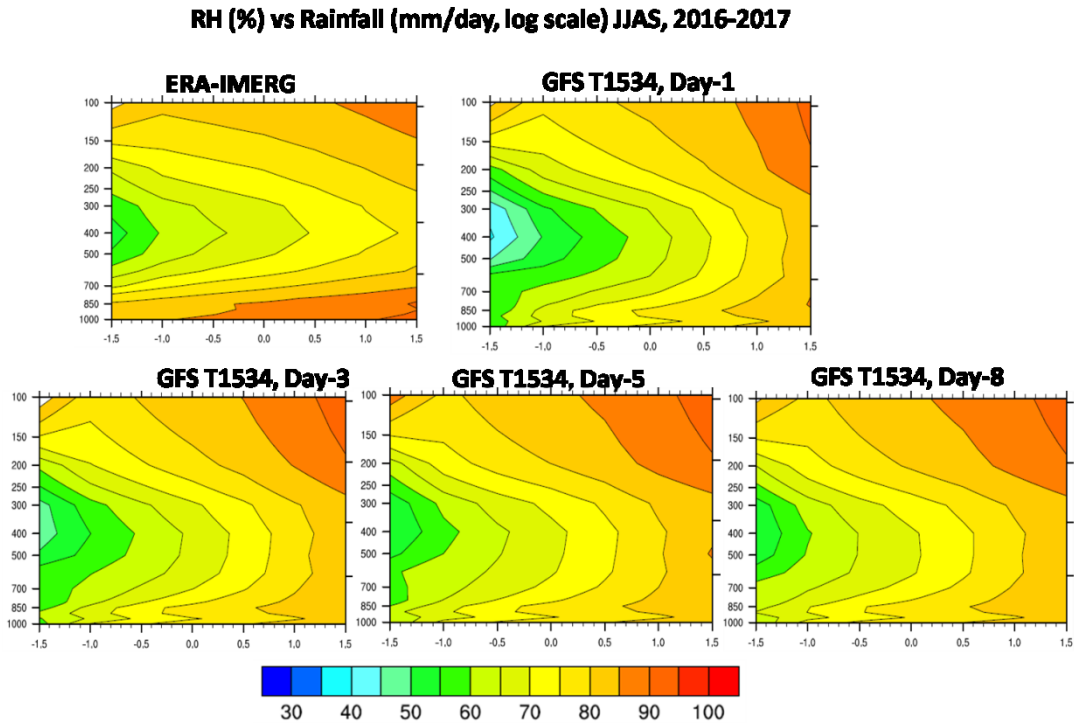

Figure 9. Vertical profile of relative humidity (shaded in %) as a function of rain rate (mm/day) over central Indian region during JJAS of 2016-2017 from observation (ERA-Interim versus IMERG, top left side) and GFS T1534 at various lead time respectively. The rain rate at the x axis is plotted in log10 scale.

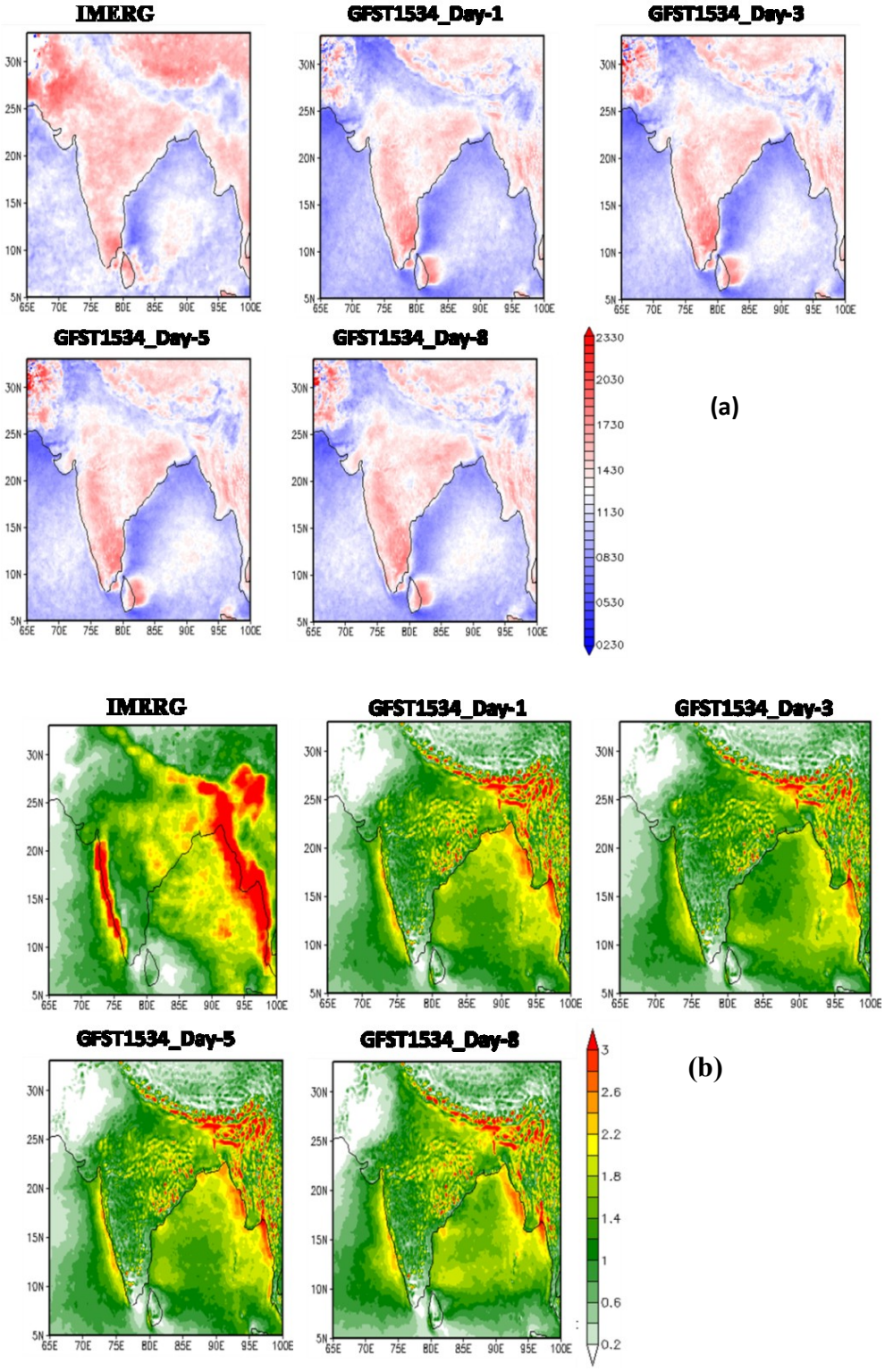

Figure 10. (a) JJAS distribution of diurnal phase (IST (h)) when maximum precipitation occurs for IMERG (top left) and GFS T1534 model forecast at different lead time respectively. (b) represents the distribution of diurnal absolute amplitude (mm/hr) defines as the difference between maximum and minimum rainfall in a day.

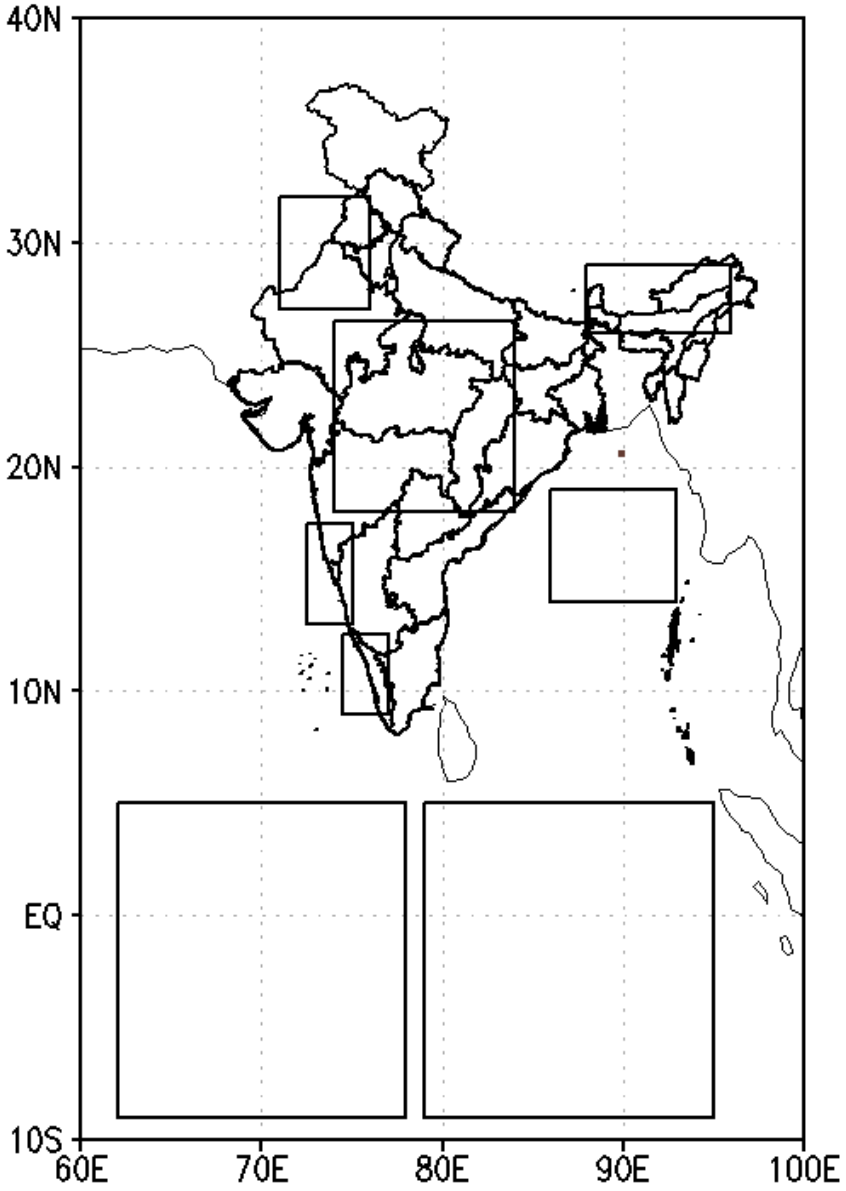

Figure 11.Selected boxes over Indian region to calculate diurnal cycle of rainfall.

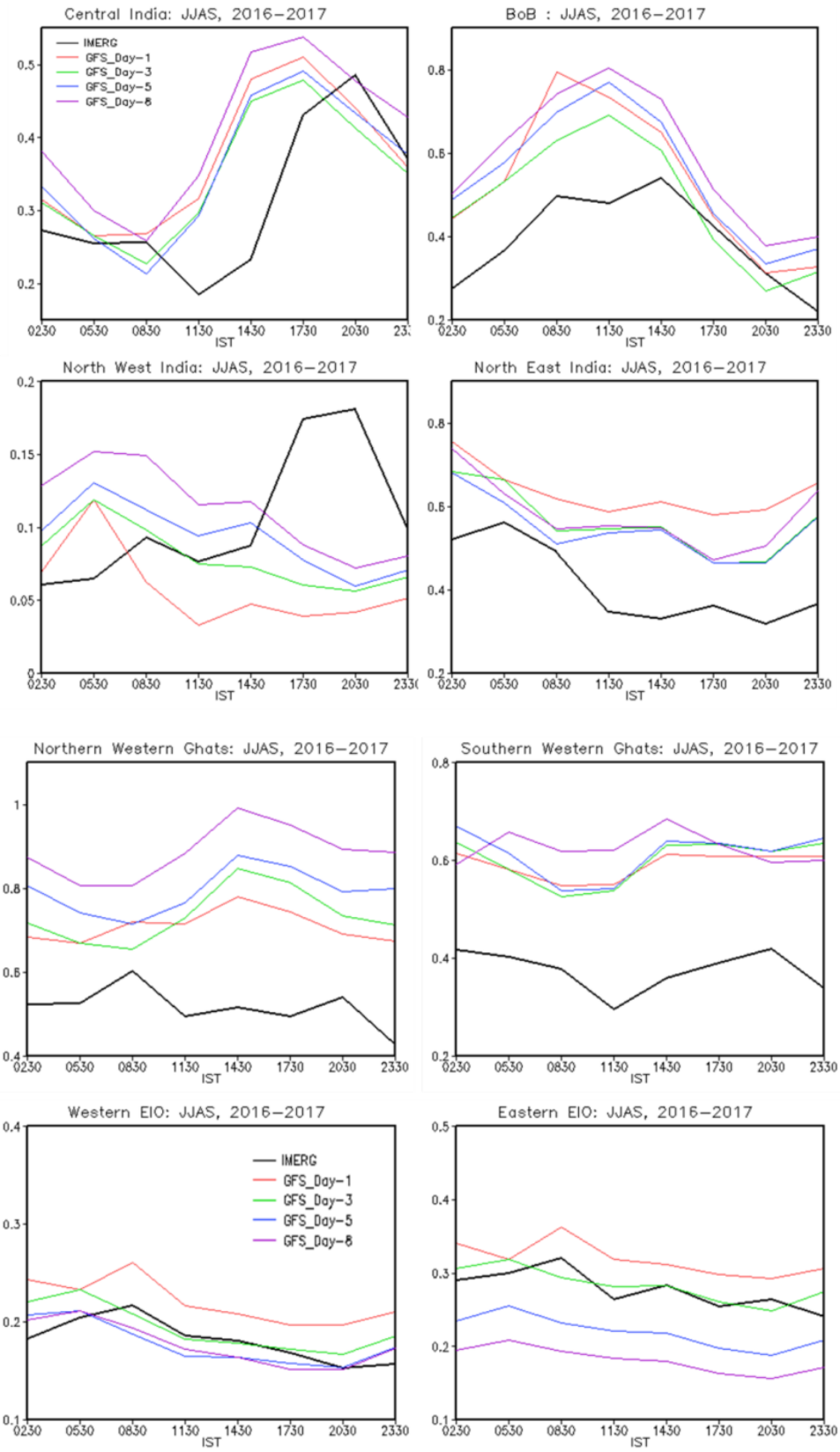

Figure 12. Diurnal cycle of rainfall (mm/hr) over different boxes as in figure 11 over Indian region as obtained from IMERG (black line) and GFS T1534 model forecast at different lead time during JJAS of 2016-2017.

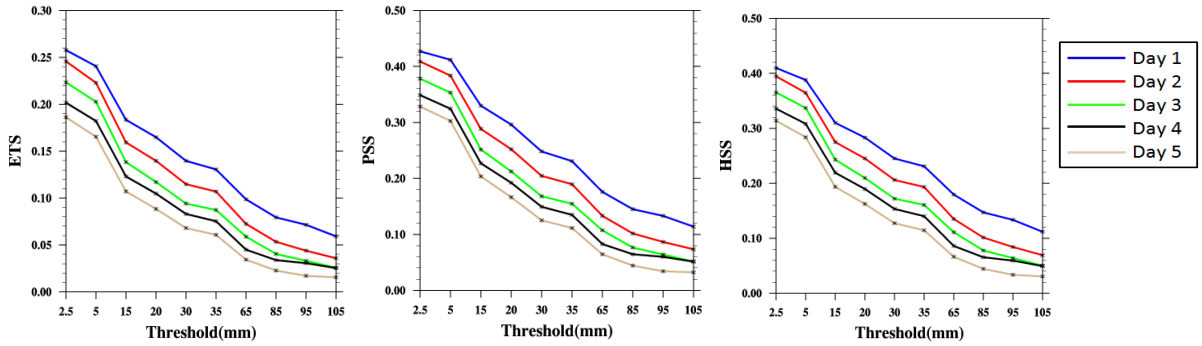

Figure 13. (a) Equitable Threat Score and (b) Peirce Skill Score (c) Heidke Skill Score of GFS T1534 for JJAS 2016-2017 for all India land grid points.

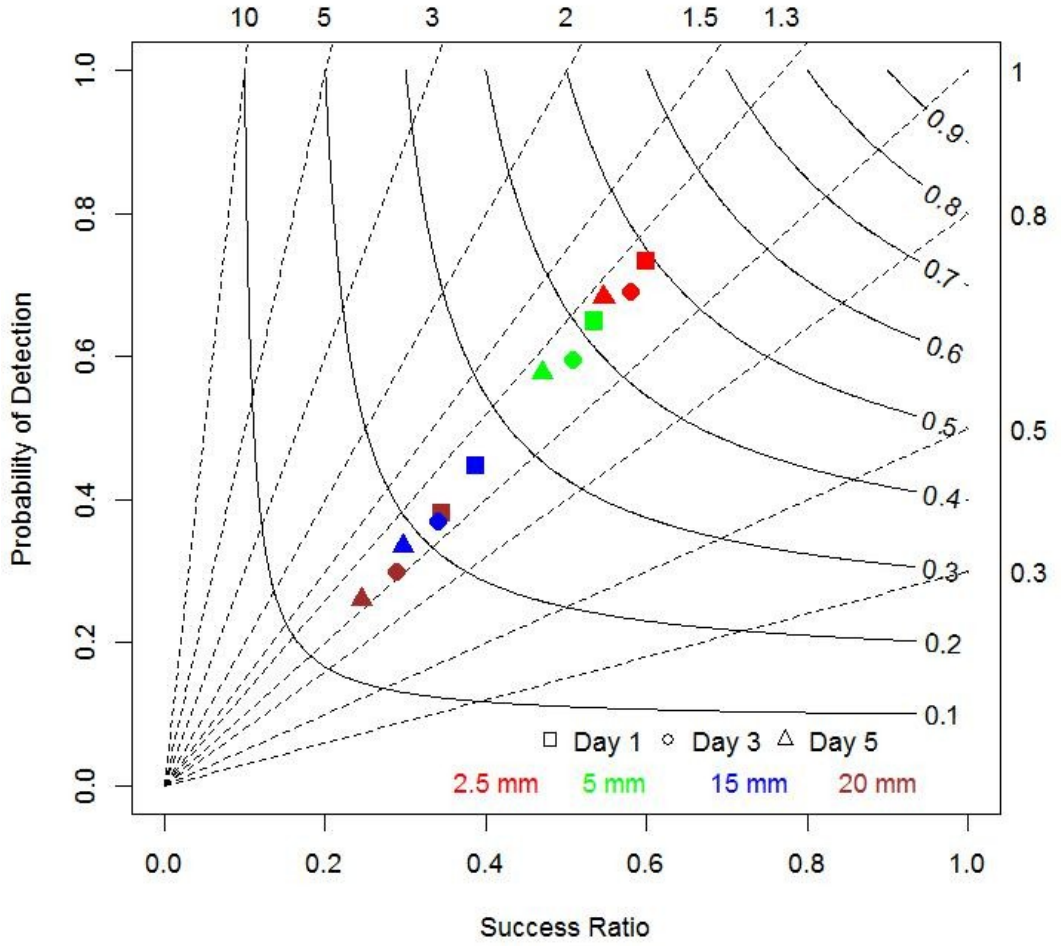

Figure 14. Figure 14. Performance diagram of GFS T1534 for JJAS 2016-2017 for all India land grid points.

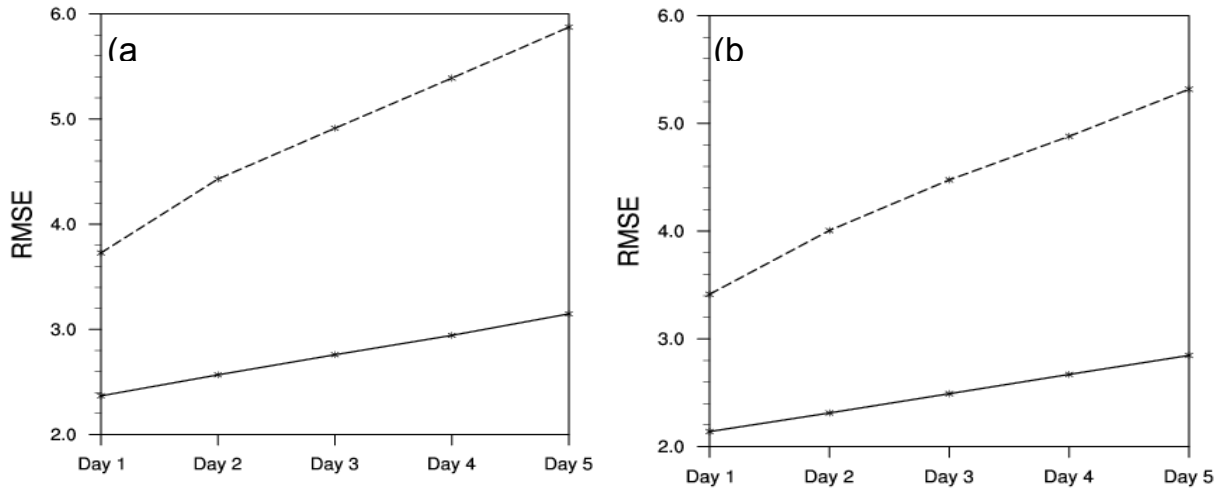

Figure 15. Root mean square error (RMSE) of (a) U component of wind at 850 hPa (solid) and at 200 hPa (dashed) (b) V component of wind at 850 hPa (solid) and at 200 hPa (dashed) for JJAS 2016-2017 for the domain 10˚S-40˚N, 50˚E-120˚E

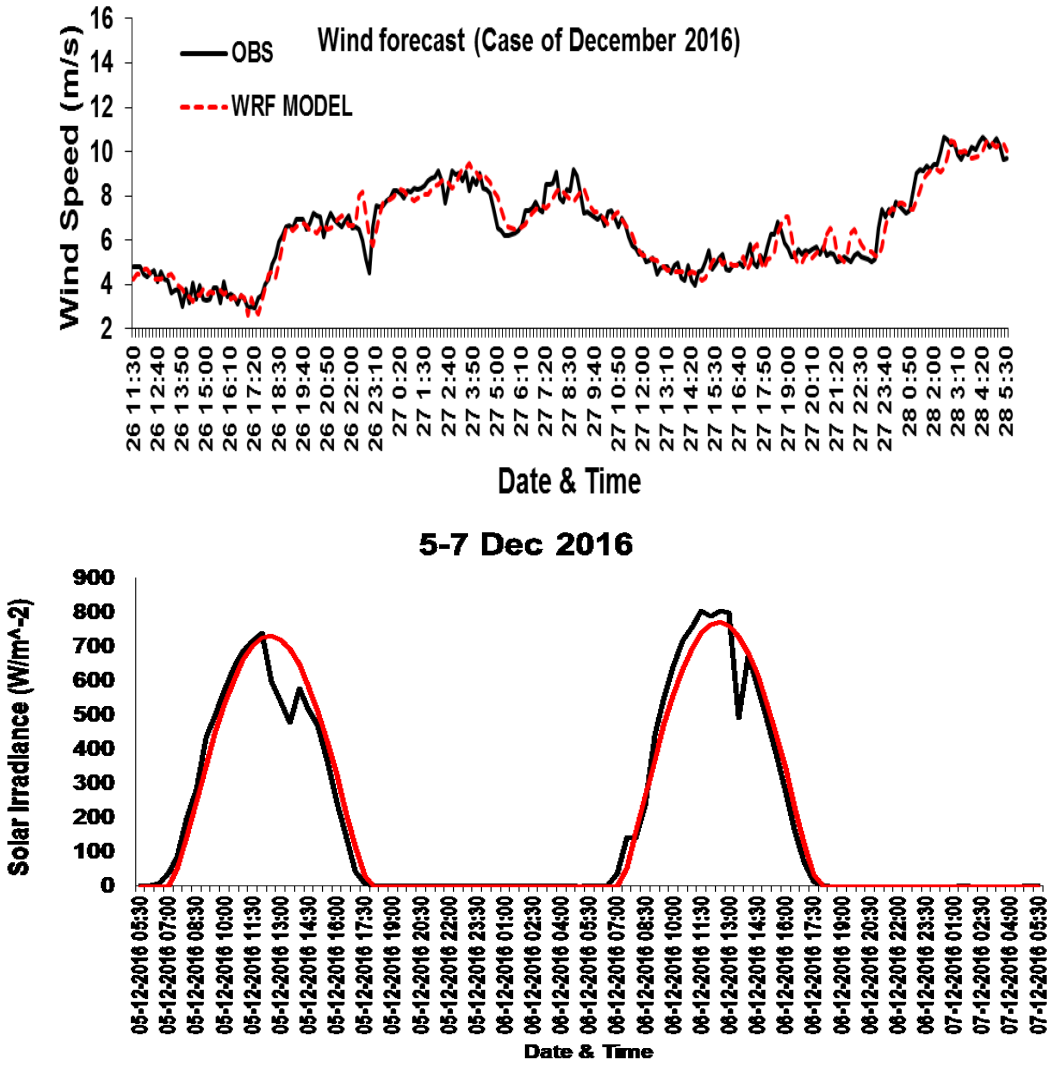

Figure 16. (a) A day ahead forecast of wind at 90m height by WRF model (red) compared with Observations (black). (b) Same as Fig 1a but forecast for solar irradiance by WRF-Solar (red).

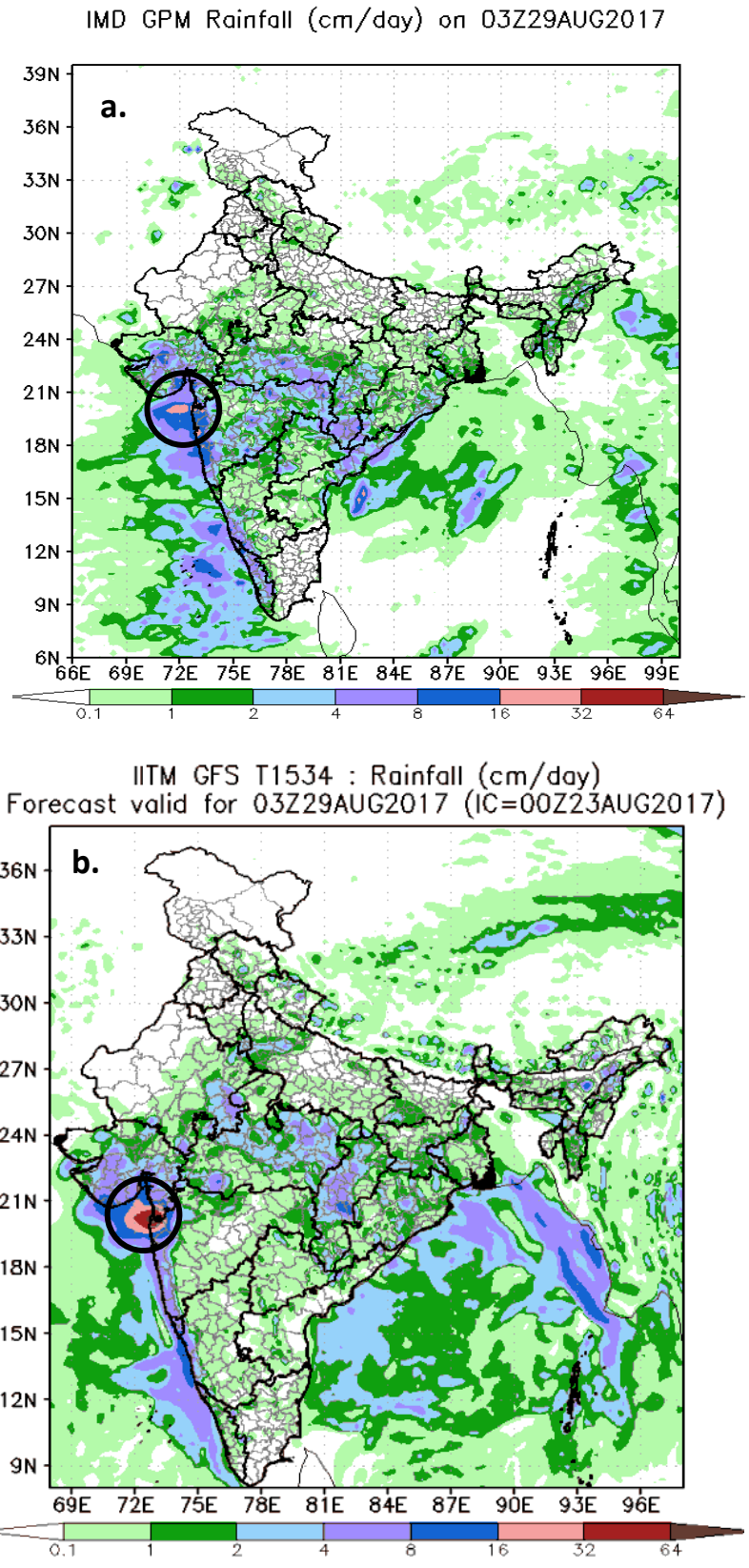

Figure 17. 24hours accumulated rainfall on 29Aug 2017 from (a) IMD-GPM (observations) (b) Model Forecast with 23Aug 2017 initial conditions. Circle denotes the location of the events.

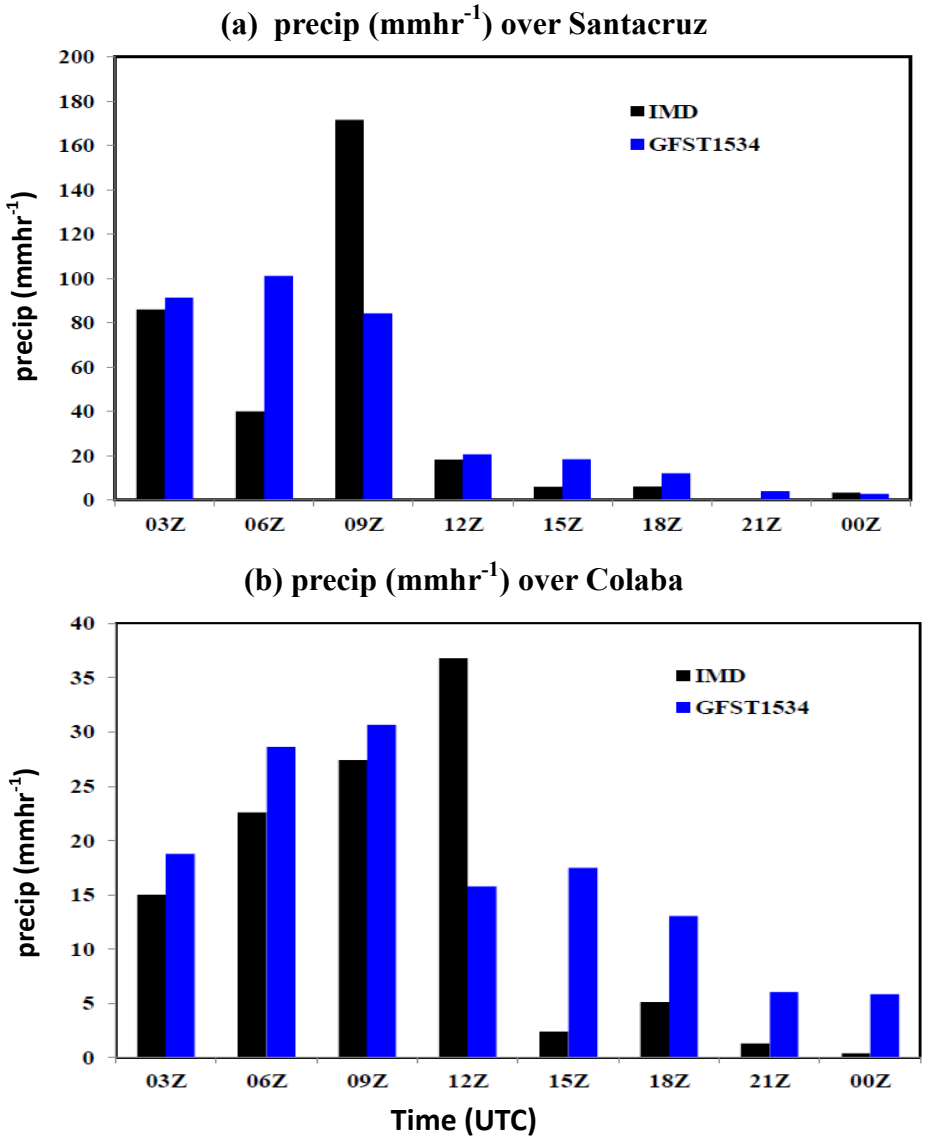

Figure 18. Time series of precipitation (mm hr^{-1}) during 29 August 2017 at three hourly interval from IMD (black color) and GFS T1534 model (blue color) forecast based on 27 August 2017 Initial condition model forecast over (a) Santacruz and (b) Colaba in Mumbai region.